

# Closed-Form Performance for Location Estimation Based on Quantized Data in Sensor Networks

Yujiao Zheng, Ruixin Niu, and Pramod K. Varshney

EECS Department, Syracuse University

Syracuse, NY 13244, U.S.A.

[yuzheng](mailto:yuzheng@syr.edu), [rniu](mailto:rniu@syr.edu), [varshney](mailto:varshney@syr.edu)@syr.edu

**Abstract** – For a large and dense sensor network, the impact of sensor density is investigated on the performance of a maximum likelihood (ML) location estimator using quantized sensor data. The ML estimator fuses quantized data transmitted from local sensors to estimate the location of a source. A Gaussian-like isotropic signal decay model is adopted to make the problem tractable. This model is suitable for situations such as passive sensors monitoring a target emitting acoustic signals. The exact Cramér-Rao lower bound (CRLB) on the estimation error is derived. In addition, an approximate closed-form CRLB by using the Law of Large Numbers is obtained. The closed-form results indicate that the Fisher information is a linearly increasing function of the sensor density. Even though the results are derived assuming a large number of sensors, numerical results show that the closed-form CRLB is very close to the exact CRLB for both high and relatively low sensor densities.

**Keywords:** Localization, location estimation, Cramér-Rao lower bound, sensor networks, quantization.

## 1 Introduction

With the significant advances in networking, wireless communications, micro-fabrication, and microprocessors, the wireless sensor network (WSN), once a futuristic technology, has become much more feasible. Due to their many applications in environmental monitoring, battlefield surveillance, and structural health management, WSNs have received considerable attention in recent years [1, 2, 3]. In the envisioned WSNs, there are a large number of inexpensive sensors which are densely deployed in a region of interest (ROI). This makes accurate intensity (energy) based object localization possible. Because signal intensity measurements are usually employed for object detection, it is very convenient and economical to utilize them to localize an object, without the need for more sophisticated and more expensive sensor functionalities, such as the direction of

arrival (DOA) or time-delay of arrival (TDOA) estimates. Since signal decays as a function of distance, signal intensity data contain the range information of the signal source. Energy-based methods have been proposed and developed in [4] for WSNs, where analog energy readings from sensors have been used to localize acoustic sources through the maximum-likelihood (ML) method. In [5], we developed an ML based object localization algorithm using only quantized signal amplitudes. Further, source localization based on quantized signals, which experience Rayleigh fading effect was investigated in [6].

Since localization is an estimation problem, the performance measure in which we are interested is the mean-squared error (MSE) of the estimate. It is well known that the Cramér-Rao lower bound (CRLB) [7], a classical result, provides the lower bound on the MSE for any unbiased estimator. In [5], we have shown that the ML localization algorithm can achieve its asymptotic performance bound, the CRLB, even with a few amplitude observations from the sensors. This implies that the theoretical CRLB is a reliable performance predictor. In [8], we have investigated the impact of the sensor density on the performance of a ML localization algorithm for a dense sensor network, where the fusion center receives analog data from the local sensors. A compact and closed-form result was derived. We have also shown that the Fisher information increases linearly with the sensor density and with the signal-to-noise ratio (SNR). In this paper, we further investigate the impact of the sensor density on the performance of a ML localization algorithm for a dense sensor network, where the fusion center receives quantized data from the local sensors. A compact result similar to that in [8] is derived.

The organization of the paper is as follows. In the next section, we formulate the problem considered in this paper. We use the same isotropic Gaussian-like signal attenuation model as in our previous work [8] and provide the statistical model for sensor observa-

tions. The ML location estimator based on quantized sensor data and its corresponding exact CRLB are derived in Section 3. In Section 4, using approximations based on the Law of Large Numbers (LLN), closed-form CRLBs are also derived for the Gaussian decay model. In Section 5, numerical examples are provided to illustrate the effectiveness of the closed-form solution that we propose. We finally conclude and discuss the ongoing work in Section 6.

## 2 Problem Formulation

As illustrated in Figure 1, we assume that a large number of sensors are deployed in the ROI, with a sensor density of  $\lambda$  sensors per unit area. The locations of sensors, denoted by  $(x_i, y_i)$  for  $i = 1, \dots, N$ , are independent realizations of a uniform distribution within the ROI, and they are assumed known to the fusion center.

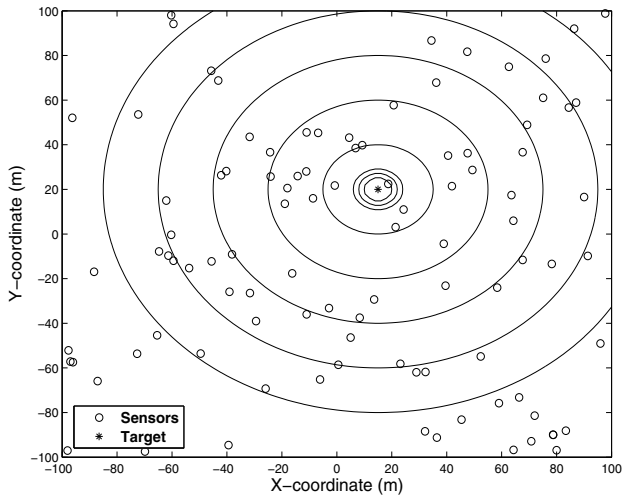


Figure 1: The signal intensity contours of a target located in a sensor field.

We make use of the same model as in [8], that is, the target emits signal power, which isotropically attenuates according to the following model:

$$a_i = g(d_i) \quad (1)$$

where  $d_i = \sqrt{(x_i - x_t)^2 + (y_i - y_t)^2}$  is the distance between the target and the local sensor  $i$ ,  $(x_t, y_t)$  are the coordinates of the target, and  $a_i$  is the received signal amplitude at sensor  $i$ . Function  $g(\cdot)$  describes how signal power decays as the distance from the target increases. In this paper, the following  $g(\cdot)$  is employed:

$$g(d) = \sqrt{P_0} e^{-\frac{\alpha d^2}{2}} \quad (2)$$

where  $P_0$  is the signal power emitted by the target at distance zero, and  $\alpha$  is a constant. We assume that  $P_0$  and  $\alpha$  are determined through experiments, and are

known to the fusion center. By adopting the Gaussian-like attenuation model described in (2), we can obtain a Fisher information matrix for any  $(x_t, y_t)$ , even when the distance between the target and a sensor is zero. Note that this is not possible for the attenuation model adopted in [5], where the signal power is inversely proportional to the distance raised to a certain power. With that model, one will get infinite Fisher information matrix elements when the distance between the target and a sensor is zero.

The signal received at a specific sensor is corrupted by an additive noise. The noises at the local sensors are i.i.d. and follow a Gaussian distribution with zero mean and variance  $\sigma^2$ :

$$s_i = a_i + n_i \quad (3)$$

where  $s_i$  is the received signal,  $a_i$  is the signal amplitude, and

$$n_i \sim \mathcal{N}(0, \sigma^2)$$

## 3 ML Location Estimator and Exact CRLB

We assume that each sensor sends quantized multibit ( $M$ -bit) data to the fusion center, which are denoted as  $\mathbf{D} = \{D_i : i = 1, \dots, N\}$  where  $D_i$  can take any discrete value from 0 to  $2^M - 1$ . We define  $L = 2^M$  and the thresholds for the  $i$ th sensor is  $\vec{\eta}_i = [\eta_{i0}, \eta_{i1}, \dots, \eta_{iL}]$ , where  $\eta_{i0} = -\infty$  and  $\eta_{iL} = \infty$ . The quantization process for the  $i$ th sensor is

$$D_i = \begin{cases} 0 & -\infty < s_i < \eta_{i1} \\ 1 & \eta_{i1} \leq s_i < \eta_{i2} \\ \vdots & \vdots \\ L-2 & \eta_{i(L-2)} \leq s_i < \eta_{i(L-1)} \\ L-1 & \eta_{i(L-1)} \leq s_i < \infty \end{cases}$$

Due to the Gaussian noise assumption, we can easily get

$$\begin{aligned} p_{il}(\vec{\eta}_i, \theta) &\triangleq p(D_i = l \mid \vec{\eta}_i, \theta) \\ &= Q\left(\frac{\eta_{il} - a_i}{\sigma}\right) - Q\left(\frac{\eta_{i(l+1)} - a_i}{\sigma}\right) \end{aligned} \quad (4)$$

where  $Q(\cdot)$  is the complementary distribution function of the standard Gaussian distribution

$$Q(x) = \int_x^\infty \frac{1}{\sqrt{2\pi}} e^{-\frac{t^2}{2}} dt \quad (5)$$

Let  $\theta \triangleq [x_t \ y_t]^T$  denote the target location. Based on the assumptions made in Section 2 and the notations above, it is easy to derive the likelihood function at the fusion center node which is given as

$$p(\mathbf{D} \mid \theta) = \prod_{i=1}^N \prod_{l=0}^{L-1} p_{il}(\vec{\eta}_i, \theta)^{\delta(D_i - l)} \quad (6)$$

where  $\delta(\cdot)$  is Kronecker delta function:

$$\delta(x) = \begin{cases} 1, & x = 0 \\ 0, & x \neq 0 \end{cases}$$

Therefore, the log-likelihood function of  $\mathbf{D}$  is as follows:

$$\ln p(\mathbf{D}|\theta) = \sum_{i=1}^N \sum_{l=0}^{L-1} \delta(D_i - l) \ln p_{il}(\vec{\eta}_i, \theta) \quad (7)$$

Now, the ML estimate of the target location is

$$\hat{\theta}_{\text{MLE}} = \arg \max_{\theta} \ln p(\mathbf{D}|\theta)$$

The CRLB on the covariance matrix of the estimation error based on sensors' observations is derived and provided in the following theorem:

**Theorem 1** *Assuming the existence of an unbiased estimator  $\hat{\theta}(\mathbf{D})$ , the CRLB is given by*

$$E \left\{ \left[ \hat{\theta}(\mathbf{D}) - \theta \right] \left[ \hat{\theta}(\mathbf{D}) - \theta \right]^T \right\} \geq \mathbf{J}^{-1} \quad (8)$$

in which  $\mathbf{J}$  is the Fisher information matrix (FIM)

$$\mathbf{J} = \sum_{i=1}^N \beta_i \mathbf{G}_i$$

where

$$\mathbf{G}_i \triangleq \begin{bmatrix} (x_i - x_t)^2 & (x_i - x_t)(y_i - y_t) \\ (x_i - x_t)(y_i - y_t) & (y_i - y_t)^2 \end{bmatrix} \quad (9)$$

$$\beta_i = \frac{\alpha^2 P_0 e^{-\alpha d_i^2}}{2\pi\sigma^2} \gamma_i$$

and

$$\gamma_i = \sum_l \frac{1}{p_{il}} \left[ e^{-\frac{1}{2} \left( \frac{\eta_{il} - a_i}{\sigma} \right)^2} - e^{-\frac{1}{2} \left( \frac{\eta_{i(l+1)} - a_i}{\sigma} \right)^2} \right]^2 \quad (10)$$

*Proof:* See Appendix A.

## 4 Closed-Form FIM and CRLB

In this section, we will derive a closed-form FIM and CRLB, by assuming the Gaussian-like signal decay model defined in (2). As we can see, the FIM provided in Theorem 1 is quite complex, since it depends on the sensors' relative positions to the target as well as the quantizer thresholds, which makes a compact solution very difficult to derive. In [8], we obtained a very simple expression for the FIM and CRLB for source localization based on analog data, by using the LLN. Here we again assume that the ROI, which is covered densely by uniformly distributed sensors, is very large. Based

on this assumption, it is reasonable to assume that for a target that is located in the ROI, the received signal is non-negligible only within a circle surrounding the target, and hence the ROI can be approximately deemed to be without boundaries. The radius of the circle around the target, denoted as  $R$ , can be determined based on (2). We assume that a received signal is negligible if  $P_i \leq \epsilon P_0$ , where  $\epsilon$  is a very small number. Then, according to (2),  $R$  can be derived as

$$R = \sqrt{\frac{\ln(1/\epsilon)}{\alpha}} \quad (11)$$

First, we investigate the (1, 1) element of the FIM

$$J_{11} = \frac{\alpha^2 P_0}{2\pi\sigma^2} \kappa_{11} \quad (12)$$

where

$$\kappa_{11} \triangleq \sum_{i=1}^N e^{-\alpha d_i^2} (x_i - x_t)^2 \gamma_i \quad (13)$$

Suppose the sensor density is high, and hence the number of sensors around the target that have non-negligible signal strength is large. In this case, we can apply the LLN [9] to approximate the summation in (13) by an integral. According to the LLN, as  $N \rightarrow \infty$

$$\frac{1}{N} \kappa_{11} \rightarrow E \left[ e^{-\alpha d_i^2} (x_i - x_t)^2 \gamma_i \right] \quad (14)$$

where the expectation is taken with respect to the sensor position  $(x_i, y_i)$ . Therefore, we have

$$\kappa_{11} \approx N \times E \left[ e^{-\alpha d_i^2} (x_i - x_t)^2 \gamma_i \right] \quad (15)$$

We assume that the sensors are uniformly distributed within a circle around the target with a radius  $R$ .

$$f(x, y) = \begin{cases} \frac{1}{\pi R^2} & (x - x_t)^2 + (y - y_t)^2 \leq R^2 \\ 0 & \text{otherwise} \end{cases} \quad (16)$$

We denote the region inside this circle as  $\mathcal{R}$  and the region inside another circle with radius  $R$  and centered at  $(0, 0)$  as  $\mathcal{R}'$ . Then,

$$\begin{aligned} \kappa_{11} &\approx \frac{N}{\pi R^2} \int \int_{\mathcal{R}} (x - x_t)^2 e^{-\alpha[(x-x_t)^2 + (y-y_t)^2]} \gamma' dx dy \\ &= \frac{N}{\pi R^2} \int \int_{\mathcal{R}'} x^2 e^{-\alpha(x^2 + y^2)} \gamma'' dx dy \\ &= \lambda \int \int_{\mathcal{R}'} x^2 e^{-\alpha(x^2 + y^2)} \gamma'' dx dy \end{aligned} \quad (17)$$

where  $\lambda$  is defined as the sensor density in the area, that is,

$$\lambda = \frac{N}{\pi R^2}$$

$\gamma'$  and  $\gamma''$  are similar to (10), except that in  $\gamma'$ ,

$$a_i^2 = P_0 e^{-\alpha((x-x_t)^2 + (y-y_t)^2)}$$

while in  $\gamma''$ ,

$$a_i^2 = P_0 e^{-\alpha(x^2+y^2)}$$

With the change of variables

$$\begin{aligned} x &= r \cos \theta \\ y &= r \sin \theta \end{aligned}$$

integration in (17) is converted from the Cartesian coordinate system to the Polar coordinate system

$$\begin{aligned} \kappa_{11} &= \lambda \int_0^R \int_0^{2\pi} e^{-\alpha r^2} r^3 \cos^2 \theta \tilde{\gamma}(r) dr d\theta \\ &= \lambda \pi \int_0^R e^{-\alpha r^2} r^3 \tilde{\gamma}(r) dr \end{aligned} \quad (18)$$

where,

$$\tilde{\gamma}(r) = \frac{\sum_{l=0}^{L-1} \left[ e^{-\frac{1}{2} \left( \frac{\eta_{il} - a(r)}{\sigma} \right)^2} - e^{-\frac{1}{2} \left( \frac{\eta_{i(l+1)} - a(r)}{\sigma} \right)^2} \right]^2}{Q \left( \frac{\eta_{il} - a(r)}{\sigma} \right) - Q \left( \frac{\eta_{i(l+1)} - a(r)}{\sigma} \right)} \quad (19)$$

and  $a(r) = \sqrt{P_0} e^{-\frac{\alpha}{2} r^2}$ . Therefore,

$$J_{11} = \frac{\lambda P_0 \alpha^2}{2\sigma^2} \int_0^R e^{-\alpha r^2} r^3 \tilde{\gamma}_{11}(r) dr$$

Following a similar procedure, we can also derive other elements in the FIM matrix:

$$J_{22} = J_{11} = \frac{\lambda P_0 \alpha^2}{2\sigma^2} \int_0^R e^{-\alpha r^2} r^3 \tilde{\gamma}_{11}(r) dr$$

$$J_{12} = J_{21} = 0$$

Therefore, we have the following theorem:

**Theorem 2** *The Fisher information matrix (FIM) for the location estimation problem with quantized data in this paper can be approximated as*

$$\mathbf{J} = \left[ \frac{\lambda P_0 \alpha^2}{2\sigma^2} \int_0^R e^{-\alpha r^2} r^3 \tilde{\gamma}_{11}(r) dr \right] \mathbf{I}_2 \quad (20)$$

where  $\mathbf{I}_2$  is a  $2 \times 2$  identity matrix.

Thus, for the quantized data case, we have obtained a result that is very similar to that for the analog data case in [8]. Theorem 2 indicates that the Fisher information is a linearly increasing function of the sensor density given the SNR. The relationship between the SNR and the Fisher information is not as obvious as the results obtained for analog data in [8], since the thresholds of the quantizer at each sensor are related to the SNR, as will be discussed in Section 5.1.

## 5 Experimental Results

In this section, we first compare the performance of the optimal quantizer (in the sense of minimizing CRLB) with the uniform quantizer, and then use the optimal quantizer that we find to perform simulations. We show that the ML estimator is efficient using quantized data when the number of quantization bits is large. The compact FIM provided by Theorem 2 will be compared to the exact FIM that is given by Theorem 1 in various scenarios.

### 5.1 Quantization Thresholds

In this subsection, we provide examples where the performance of the optimal quantizer is compared to that of the uniform quantizer. We assume that the target is located at  $[0 \ 0]$ , sensors are uniformly deployed in a square with side  $b$ , which is large enough so that the signal strength is negligible at the boundary of the square. The parameters are chosen as  $\alpha = 1$ ,  $\sigma = 1$ ,  $P_0 = 10000$ . The SNR is defined as  $\text{SNR} = P_0/\sigma^2$ . In order to find the optimal quantizer thresholds, we assume that the fusion center knows all the sensor locations.

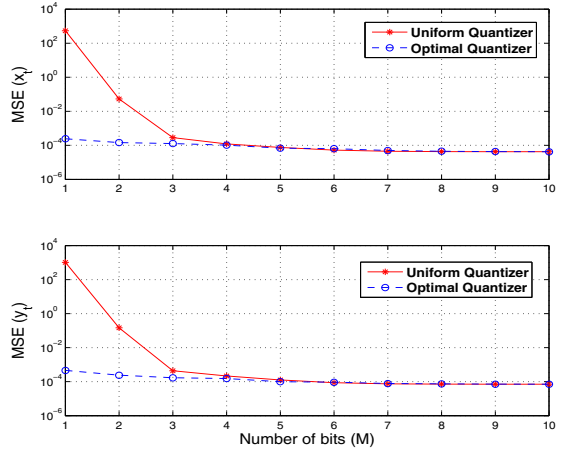


Figure 2: The CRLBs as a function of number of bits  $M$ .

In Figure 2,  $\text{SNR} = 40 \text{ dB}$ , for the first 2 bits, the optimal quantizer has much better performance (its CRLB is much lower than that of the uniform quantizer). As the number of bits increases, the two quantizer design schemes lead to almost the same performance. In the rest of the paper, the optimal quantizer will be used in the numerical examples. Note that the SNR  $P_0/\sigma^2$  is defined to be the SNR at zero distance, and the signal decays rapidly as the distance from the target increases. Therefore, 40 dB is a relatively modest SNR value.

## 5.2 ML Estimator

In this subsection, we show that the ML estimator is efficient for a large number of bits  $M$ . In the simulation, we fix the sensor density  $\lambda = 1$  in the  $b \times b$  square region, and then uniformly deploy the sensors in this region. In order to find the global maximum in ML estimation, we first employ a grid search to find a coarse maximum point. Then, starting from that point, we use Matlab's FMINCON to find the maximum point.

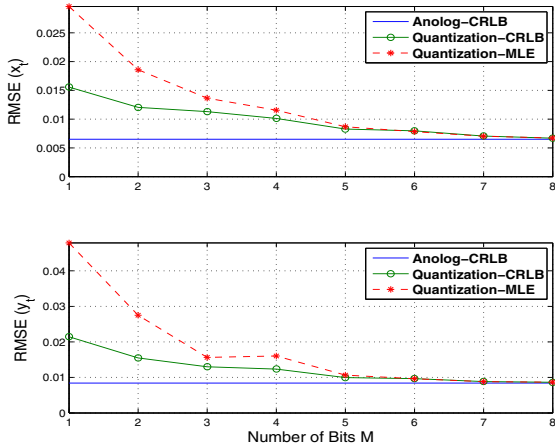


Figure 3: Root mean square error (RMSE) as a function of number of bits  $M$ . SNR = 40dB.

In Figure 3, we can observe that the gap between the CRLB of the quantized data and that of the analog data decreases rapidly as the number of bits  $M$  increases. Further, the root mean squared error (RMSE) of the MLE based on quantized data quickly converges to its CRLB when  $M$  increases. Therefore, the CRLB of the quantized data (Theorem 1) is a tight bound for the ML estimator derived in the paper, especially for a large  $M$ .

## 5.3 Approximate Closed-Form CRLB

In this experiment, we compare the compact FIM provided by Theorem 2 to that given by Theorem 1. We calculate the compact FIM provided by Theorem 2. We assume that the ROI is very large and the target is located at the center of the ROI without loss of generality. At the boundary of the ROI, which is a square with side  $b$ , the signal reduces to  $1.8 \times 10^{-35} P_0$ . A total of  $\lambda b^2$  sensors have been randomly deployed in the ROI, whose positions follow identical and independent (i.i.d.) uniform distribution within the ROI. The exact FIM is obtained via one Monte-Carlo run, meaning that only one set of realizations of the sensor positions are used. It can be shown that on the average the number of sensors whose signal power is greater than  $\epsilon P_0$  is

$$N = \lambda \pi R^2 = \frac{\lambda}{\alpha} \pi \ln(1/\epsilon) \quad (21)$$

From the above equation, it is clear that this number  $N$  is determined by  $\frac{\lambda}{\alpha}$ , for a fixed  $\epsilon$ . We define the normalized sensor density as  $\lambda' = \lambda/\alpha$ . It will be sufficient to just study cases with different  $\lambda'$ . In this experiment, we set  $\alpha = 1$ . Further, to compare the off-diagonal elements, we define a quantity analogous to the correlation coefficients for the covariance matrix [9]:

$$\rho = \frac{J_{12}}{\sqrt{J_{11}J_{22}}}$$

which is the off-diagonal element normalized by the square root of the product of the diagonal elements. This quantity captures the ‘‘correlation’’ between the two diagonal elements. In Figure 4, the elements of the FIM calculated by the exact and approximate methods for a binary quantizer ( $M = 1$ ) have been compared. As we can see, the approximate Fisher information increases linearly as sensor density increases, and the exact FIM oscillates around that obtained using the compact expression. Although convergence is not obvious in the top two figures in Figure 4, we can observe the trend from the bottom figure. That is, when the sensor density increases, the magnitude of the correlation between the two diagonal elements in the FIM decreases. The convergence is much more obvious in Figure 5. In Figure 5, the trace of the CRLB matrix is provided as a function of  $\lambda$ . Note that this entity gives the CRLB on the summation of the MSEs of the target’s two coordinates  $x_t$  and  $y_t$ . We can see that the estimation accuracy improves as the sensor density increases.

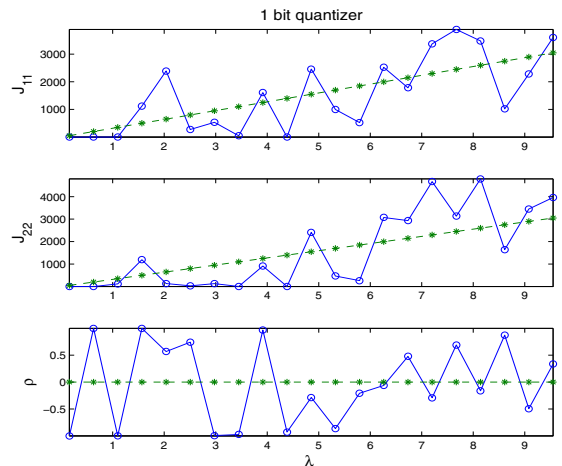


Figure 4: Elements of FIM as a function of sensor density  $\lambda$ . Solid line + circle: Exact FIM; Dashed line + star: Approximate FIM calculated using Theorem 2. SNR = 40dB and  $M = 1$ .

We also obtain the results for a 3-bit quantizer, as shown in Figures 6 and 7. The exact FIM converges to the approximate one very quickly. Thus, the result

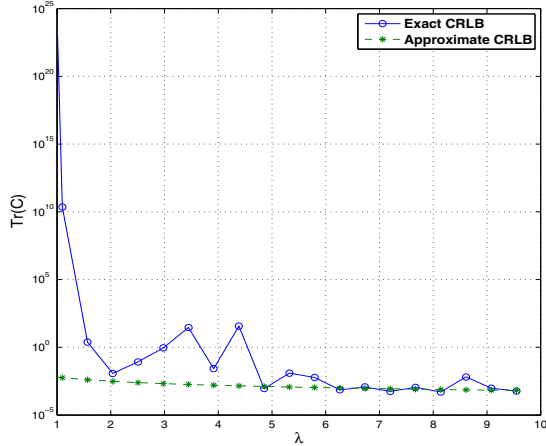


Figure 5: Trace of the CRLB matrix as a function of sensor density  $\lambda$ . Solid line + circle: Exact CRLB; Dashed line + star: Approximate CRLB calculated using Theorem 2. SNR = 40dB, and  $M = 1$ .

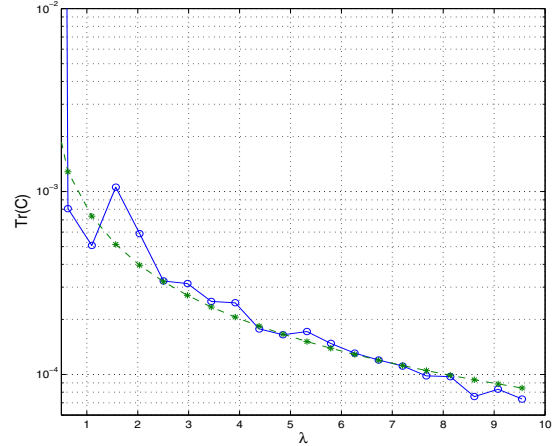


Figure 7: Trace of the CRLB matrix as a function of sensor density  $\lambda$  (3-bit quantizer). Solid line + circle: Exact CRLB; Dashed line + star: Approximate CRLB calculated using Theorem 2. SNR = 40dB and  $M = 3$ .

given by Theorem 1 quickly converges to that given by Theorem 2.

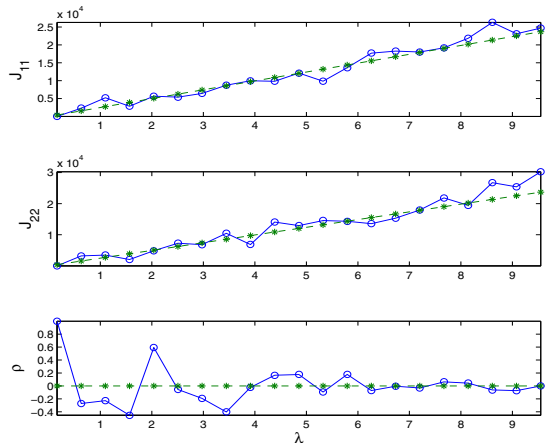


Figure 6: Element of FIM as a function of sensor density  $\lambda$ . Solid line + circle: Exact FIM; Dashed line + star: Approximate FIM calculated using Theorem 2. SNR = 40dB and  $M = 3$ .

## 6 Conclusion

In this paper, we have investigated the impact of sensor density on a ML localization algorithm. The algorithm utilizes the received quantized signal amplitudes from local sensors to estimate the coordinates of the target. The signal emitted by the target has been assumed to decay isotropically following a Gaussian-like attenua-

tion model. Besides the exact CRLB, we have also derived a closed-form and compact approximation to the CRLB based on the application of the LLN. This closed-form result has helped us gain insights on the relationship between the localization performance and the sensor density and SNR. Namely, the Fisher information is linear in the sensor density given the SNR. Numerical experiments have been conducted and the effectiveness of the approximation has been verified. In this paper, the optimal quantizer has been derived, by assuming the knowledge of the sensor locations at the fusion center. Our future research will be to derive the optimal quantizer without this knowledge at the fusion center. Further, research work will be extended to cases where other signal attenuation models are assumed.

## A Proof of Theorem 1

As we know, the FIM can be obtained as follows:

$$\mathbf{J} = -E [\nabla_{\theta} \nabla_{\theta}^T \ln p(\mathbf{D}|\theta)]$$

First, we derive the (1,1) element of  $\mathbf{J}$ . Taking partial derivative twice of both sides of (7) with respect to  $x_t$ , we have

$$\begin{aligned} \frac{\partial^2 \ln p(\mathbf{D}|\theta)}{\partial x_t^2} &= \sum_i \sum_l \frac{\delta(D_i - l)}{p_{il}} \frac{\partial^2 p_{il}}{\partial x_t^2} \\ &- \sum_i \sum_l \frac{\delta(D_i - l)}{p_{il}^2} \left[ \frac{\partial p_{il}}{\partial x_t} \right]^2 \end{aligned} \quad (22)$$

Since

$$E [\delta(D_i - l)] = p_{il}(\vec{\eta}, \theta)$$

we have

$$E \left[ \frac{\partial^2 \ln p(\mathbf{D}|\theta)}{\partial x_t^2} \right] = - \sum_i \sum_l \frac{1}{p_{il}} \left[ \frac{\partial p_{il}}{\partial x_t} \right]^2 \quad (23)$$

where

$$\begin{aligned} \frac{\partial p_{il}}{\partial x_t} &= \frac{\partial}{\partial x_t} \left[ Q \left( \frac{\eta_{il} - a_i}{\sigma} \right) - Q \left( \frac{\eta_{i(l+1)} - a_i}{\sigma} \right) \right] \\ &= \frac{e^{-\frac{1}{2} \left( \frac{\eta_{il} - a_i}{\sigma} \right)^2} - e^{-\frac{1}{2} \left( \frac{\eta_{i(l+1)} - a_i}{\sigma} \right)^2}}{\sqrt{2\pi}\sigma} \frac{a_i \alpha (x_i - x_t)}{\sqrt{2\pi}\sigma} \end{aligned}$$

Therefore, it is easy to derive that

$$\mathbf{J}_{11} = -E \left[ \frac{\partial^2 \ln p(\mathbf{D}|\theta)}{\partial x_t^2} \right] \quad (24)$$

$$= \sum_i \frac{a_i^2 \alpha^2}{2\pi\sigma^2} (x_i - x_t)^2 \gamma_i \quad (25)$$

where

$$\gamma_i = \sum_l \frac{1}{p_{il}} \left[ e^{-\frac{1}{2} \left( \frac{\eta_{il} - a_i}{\sigma} \right)^2} - e^{-\frac{1}{2} \left( \frac{\eta_{i(l+1)} - a_i}{\sigma} \right)^2} \right]^2 \quad (26)$$

Following a similar procedure, other elements of  $\mathbf{J}$  can be derived easily. Here, we skip their derivation.

## Acknowledgment

This work was supported in part by U.S. Army Research Office under Award W911NF-09-1-0244, and by New York State Center for Advanced Systems and Engineering (CASE).

## References

- [1] S. Kumar, F. Zhao, and D. Shepherd Eds., "Special issue on collaborative signal and information processing in microsensors networks," *IEEE Signal Processing Magazine*, vol. 19, no. 2, Mar. 2002.
- [2] H. Gharavi and S. Kumar Eds., "Special issue on sensor networks and applications," *Proceedings of the IEEE*, vol. 91, no. 8, August 2003.
- [3] A. Sayeed, D. Estrin, G. Pottie, and K. Ramchandran Eds., "Special Issue on Self-Organizing Distributed Collaborative Sensor Networks," *IEEE Journal on Selected Areas in Communications*, vol. 23, no. 4, April 2005.
- [4] X. Sheng and Y.H. Hu, "Maximum likelihood multiple-source localization using acoustic energy measurements with wireless sensor networks," *IEEE Trans. Signal Process.*, vol. 53, no. 1, pp. 44–53, Jan. 2005.
- [5] R. Niu and P.K. Varshney, "Target location estimation in sensor networks with quantized data," *IEEE Trans. on Signal Process.*, vol. 54, no. 12, pp. 4519–4528, December 2006.
- [6] R. Niu and P. K. Varshney, "Source Localization in Sensor Networks with Rayleigh Faded Signals," in *Proceedings of the 2007 IEEE International Conference on Acoustics, Speech, and Signal Processing*, Honolulu, Hawaii, April 2007, vol. III, pp. 1229–1232.
- [7] H.L. Van Trees, *Detection, Estimation and Modulation Theory*, vol. 1, Wiley, New York, 1968.
- [8] R. Niu and P. K. Varshney, "Closed-Form Performance For Location Estimation Based on Fused Data in a Sensor Network," in *Proc. the 12th International Conference on Information Fusion*, Seattle, Washington, July 2009.
- [9] A. Papoulis, *Probability, Random Variables, and Stochastic Processes*, McGraw-Hill, New York, NY, 1984.